Thin Film Structure of Symmetric Rod−Coil Block Copolymers

Bradley D. Olsen,† Xuefa Li,‡ Jin Wang,‡ and Rachel A. Segalman*,†

Department of Chemical Engineering, University of California at Berkeley, Berkeley, California 94720, and Materials Science Division, Lawrence Berkeley Laboratory, and Advanced Photon Source, Argonne National Lab, Argonne, Illinois 60439

Received October 18, 2006; Revised Manuscript Received February 6, 2007

ABSTRACT: Poly(alkoxyphenylenevinylene-*b*-isoprene) (PPV-*b*-PI) rod−coil block copolymers demonstrate novel structures due to the rodlike PPV block. Thin films of the polymers self-assemble into lamellar microphases upon thermal annealing with the lamellae oriented primarily parallel to the substrate. The parallel lamellae show symmetric wetting of PI at both the substrate and vacuum interfaces. Grains of lamellae with parallel orientation are characterized by irregular polygon shapes and are bounded by defect regions where the lamellae are oriented out of the plane of the film. Grazing-incidence small-angle X-ray scattering (GISAXS) shows that these out-of-plane lamellae are strongly oriented perpendicular to the film. The perpendicular lamellae are much straighter than those typically observed in coil−coil block copolymers due to the high bending energy of the liquid crystalline rod nanodomains. Islands or holes form in the films, and domain spacings estimated from the island/hole heights are equal to the bulk domain spacing. The perpendicular "defect" lamellae mediate the change in thickness required to transition between islands or holes and the surrounding region. Increasing film thickness results in an increasing fraction of the surface covered by perpendicular lamellae, presumably due to limited penetration of the substrate orienting field into the film. At great enough thickness total reorientation of the lamellar structure from parallel to perpendicular orientation at the vacuum interface is observed.

Introduction

The self-assembly and ordering of block copolymer thin films have been widely investigated for applications such as nanopatterning and nanolithography,[1−3] where the ability of block copolymers to form 10 nm structures suggests low-cost techniques for fabricating arrays and lines. Most research to date has focused on films where both blocks of the polymer have a Gaussian coil morphology. However, many functional polymers, such as semiconducting polymers, have a persistence length much longer than their contour length. These polymers assume a rodlike shape, so block copolymers containing them often have a rod−coil molecular shape. In organic electronics, control of the interfacial structure and morphology on the 10 nm length scale of exciton diffusion is critical to optimize the optical and electronic properties,[4−6] and patterning and morphological control of rod−coil block copolymers are being actively pursued for several selected applications.[7,8] However, incorporating a rodlike block fundamentally changes the thermodynamics governing self-assembly. Whereas the phase diagram of a bulk coil−coil block copolymer is parametrized primarily by the volume fraction of one block and the Flory−Huggins interaction parameter, additional complexities exist in rod−coil systems due to liquid crystalline rod−rod interactions and the geometric mismatch between the long rod and the wide coil.[9,10] The interplay between these thermodynamic forces results in a number of self-assembled structures in rod−coil block copolymers that are not seen in coil−coil block copolymers, such as the lyotropically self-assembled zigzag or arrowhead phases[11,12] and the strip and puck phases observed in systems with oligomeric rods.[13] In the weakly segregated regime, a phase diagram has been developed showing that lamellar phases are the most stable ordered phase in this limit.[10,14]

In order to be used in many applications, rod−coil block copolymers must be patterned into thin films. Confinement of block copolymers between planar solid or air interfaces results in complex behavior due to surface segregation effects and the discrete size of the block copolymer spacing.[1,2] In most coil−coil block copolymer films, the surface energy is such that one block prefers each interface, and the material will rearrange to preferentially place that block at the interface. Even in the simplest case of a lamellar block copolymer, this leads to a variety of morphologies depending on the film thickness and whether both interfaces prefer the same block (symmetric wetting) or different blocks (asymmetric wetting).[2,15,16] When one block preferentially segregates to each interface, the lamellae are oriented primarily parallel to the film surface, whereas perpendicular orientation is observed on nonpreferential surfaces.[17−20] Surface segregation and geometric confinement may also induce a surface reconstruction of the block copolymer microphase.[21−23] In general, these effects decay with increasing distance from the film surface. Geometry also plays a role in thin film self-assembly through the dual length scales of the film thickness and the block copolymer domain spacing. If the natural repeat spacing of a parallel oriented block copolymer is incommensurate with the film thickness, the film segregates excess material to the top surface to form an incomplete layer.[24,25] This layer has a thickness equal to the natural period of the block copolymer and is referred to as an island layer if the material forms discrete patches or a hole layer if it is closer to continuous.

Self-assembly in rod−coil block copolymer films has been studied much less extensively than coil−coil films. Aggregates or micelles that form in solution are often kinetically trapped and deposited into the film.[26−30] In thicker films the deposited aggregates may pack into a regular structure such as layers[30] or ribbonlike aggregates.[31] The final film morphology may be influenced by the lyotropic nature of self-assembly, resulting in the zigzag morphology[32] or kinetically trapped arrangements

* Corresponding author. E-mail: segalman@berkeley.edu.
† University of California at Berkeley and Lawrence Berkeley Laboratory.
‡ Argonne National Lab.

10.1021/ma062402i CCC: $37.00 © 2007 American Chemical Society
Published on Web 04/03/2007

Table 1. Molecular Properties of PPV-*b*-PI Block Copolymers

polymer	M_n(PPV) (g/mol)	M_n(PI) (g/mol)	coil fraction	N	R_g/L	ODT (°C)	l(SAXS) (nm)	l(AFM) (nm)	reorientation thickness
PPVbPI42-LMW	3500	2400	0.42	82	0.245	110	13.9	14.0	9l (125 nm)
PPVbPI59-LMW	3500	4700	0.59	116	0.345	120	17.0	16.9	8l (136 nm)
PPVbPI41-HMW	5300	3400	0.41	120	0.196	210	15.0	15.4	
PPVbPI57-HMW	5600	6600	0.57	172	0.257	190	21.8	22.4	
PPVbdPI58-HMW	5100	6300	0.58	161	0.280	>200	20.8	21.7	

of nanodomains.[33] Drying through lyotropic liquid crystalline phases can also kinetically trap defects that form in intermediate nematic[34,35] or cholesteric phases.[36] While these solution self-assembly techniques allow a wide variety of morphologies to be accessed in rod−coil block copolymer films, the strong dependence of the morphology on processing history means that little can be understood about the effects of geometric confinement, surface segregation, and grain growth on structure in these systems. Microphase separation has also been achieved by thermal annealing of films,[37] although with too little long-range order for easy structural characterization.[7,38]

Because of incommensurability between the average film thickness and the natural domain spacing of block copolymers, island or hole morphologies have also been observed in submonolayer films of rod−coil oligomers and polymers.[26,31,39,40] Oligomeric rod−coil systems formed islands or holes similar to those observed in coil−coil block copolymers in films thicker than a single monolayer,[41] but changes in the solvent evaporation conditions result in the coexistence of ribbonlike aggregates with the islands or holes. In other cases, the islands were composed of aggregates of ribbons[26,31] or micelles[29] of a constant height. Even less theoretical work has been done to understand equilibrium self-assembly in rod−coil block copolymer thin films. Pereira and Williams performed calculations for rod−coil molecules confined between two hard interfaces with varying separation between the surfaces and interfacial strengths.[42] They found that when the film thickness is incommensurate with the block copolymer domain spacing, incommensurability is accommodated through changes in the rod tilt angle relative to the lamellar normal as well as reorientation of lamellar domains to be perpendicular to the substrate.[42] This reorientation may persist even as the film thickness becomes 10 times larger than the block copolymer domain spacing.

In this study, we illustrate the impact of surface segregation and geometric confinement on self-assembly in symmetric rod−coil block copolymer systems. Block copolymer films of varying thicknesses, molecular weights, and coil fractions are shown to impact grain shape, island or hole formation, interfacial segregation, and microdomain orientation in rod−coil block copolymer thin films. Unusual structures result from the high bending rigidity of the liquid crystalline nanodomains, and preferential segregation to the film interfaces induces island and hole formation. Microdomain orientation at the vacuum interface changes with increasing thickness: lamellar microdomains are oriented primarily parallel to the film in thin films, while lamellae are increasingly oriented perpendicular to the vacuum interface in thicker films.

Experimental Methods

Poly(2,5-di(2′-ethylhexyloxy)-1,4-phenylenevinylene)-*b*-polyisoprene (PPV-*b*-PI) block copolymers were synthesized as described previously.[14] Using the weakly segregated PPV-*b*-PI system where the order−disorder transition (ODT) and bulk phase behavior are known gives an added understanding of the microphase structure and kinetic barriers to self-assembly in films.

Table 1 lists molecular weights and coil fractions for the materials studied. The number of repeat units, N, is calculated on the basis of a reference volume of one isoprene repeat unit, and the ratio of the coil block radius of gyration to the rod block length, R_g/L, represents the degree of conformational asymmetry between the rod and coil. The polyisoprene block was synthesisized anionically in benzene, resulting in ∼93% 1,4 addition as determined by ^{1}H NMR. PPVbdPI58-HMW was synthesized from perdeuterated isoprene monomer (purchased from Polymer Source, 98% isotopic enrichment) to produce a deuterated polyisoprene block. Because of trace THF in the purchased monomer, the deuterated polyisoprene block contains ∼65% 1,4 addition, as determined by ^{2}H NMR. The polydispersity of the PPV blocks ranged between 1.05 and 1.17, and the polydispersities of all the PI blocks were less than 1.05. All of the polymers formed lamellar phases in the bulk, as determined by small-angle X-ray scattering (SAXS) and transmission electron microscopy (TEM), as published elsewhere.[14,43] The bulk domain spacings measured by SAXS are summarized in Table 1.

Samples were prepared for scanning force microscopy (SFM) and grazing-incidence small-angle X-ray scattering (GISAXS) by spin-casting polymers from toluene solution onto (100) silicon wafers with a native oxide surface. The wafers were used as received from University Wafer (Boston, MA). Concentrations from 5 to 40 mg/mL and spin speeds between 900 and 6000 rpm were used to achieve film thicknesses ranging from 7 to 350 nm. Prior to annealing, the films were structureless, and samples were annealed at 80 °C under vacuum for 24 h unless otherwise noted. Sample thicknesses were measured prior to thermal annealing using a Sentech SE400 ellipsometer with a 632.8 Å laser. Film thicknesses have been nondimensionalized in terms of the bulk domain spacing of each polymer, and the symbol l is used to represent the thickness of a single domain spacing. SFM samples were analyzed on a Digital Instruments MultiMode AFM operating in tapping mode.

GISAXS experiments were performed at beamline 8-ID-E of the Advanced Photon Source using an experimental geometry similar to those described previously.[44,45] Experiments were performed using a 1.664 Å X-ray beam with a width of 100 μm and a height of 50 μm. Data were recorded on a 2D CCD detector, and the sample-to-detector distance was 2.27 m. Data were acquired for 30 s per frame at an incident angle of 0.175° (above the critical angle for these films such that the X-ray penetration depth was much larger than the film thickness), and three frames from different spots on the sample were added to generate the scattering plot. Scattering angles were converted into q-space accounting for the planarity of the detector. The q_z axis was calculated using the direct beam as the reference beam and holding q_{xy} fixed at zero. The q_{xy} axis was similarly calculated holding q_z fixed at zero. Although the geometry of the grazing incidence experiment creates distortions in q-space, the q_z and q_{xy} axes approximate a Cartesian coordinate system to a high degree of accuracy in the small-angle regime. Scattering intensities are reported in arbitrary units.

Samples for dynamic secondary ion mass spectrometry (dSIMS) were prepared by spin-casting the deuterated block copolymer PPVbdPI58-HMW onto a 300 nm thick layer of thermal oxide on a Si wafer to insulate the film.[46] Film thicknesses were prepared such that islands or holes would not form, and samples were annealed for 24 h at 160 °C under vacuum. Depth profiles were acquired using a Physical Electronics 6650 dynamic SIMS. A 2 kV, 30 nA beam of O_2^+ ions was rastered over the sample to etch a 200 μm × 200 μm crater. Charge neutralization was maintained with a 0.6 eV defocused electron beam. Atomic abundances have been normalized by the carbon signal, and the etch rate was converted to a quantitative depth scale using the known lamellar

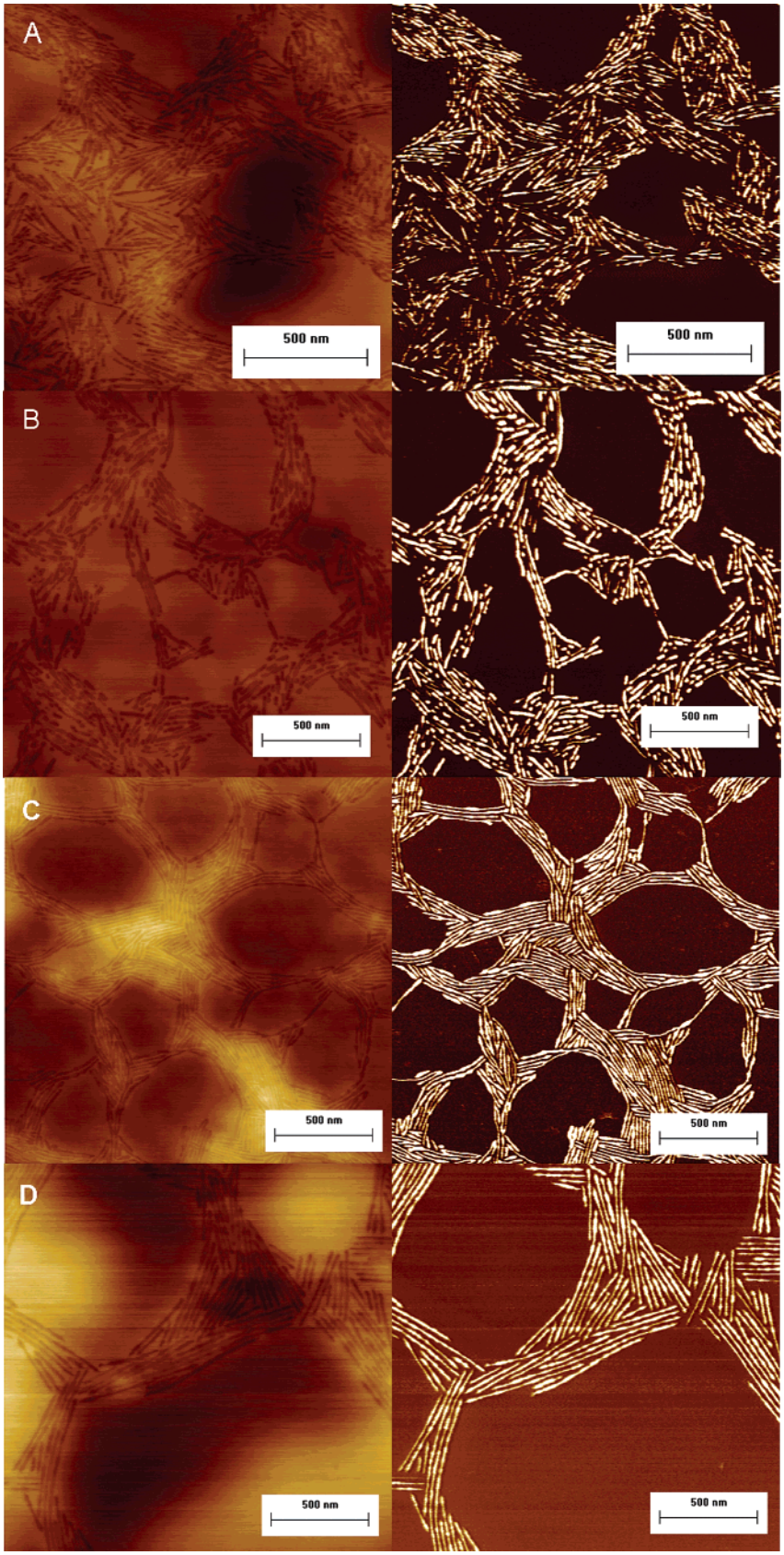

Figure 1. Nanophase structure in symmetric rod−coil block copolymer thin films. Thin films self-assemble into lamellar structures with lamellae oriented both parallel to the substrate (featureless regions) and out of the plane of the substrate (regions of alternating light and dark stripes). Phase images (right) clearly show PPV-rich (light) and PI-rich (dark) nanodomains. The high moduli of the liquid crystalline nanodomains leads to out-of-plane lamellae with long persistence lengths. Lamellae oriented parallel to the film grow into grains with irregular polygon shapes, and the straight edges are defined by the out-of-plane lamellae. While grain shape is similar for all polymers, higher molecular weight systems exhibit better ordering. (A) PPVbPI42-LMW annealed at 80 °C, 6.5*l* thick; (B) PPVbPI59-LMW annealed at 80 °C, 5.2*l* thick; (C) PPVbPI41-HMW annealed at 160 °C, 4.1*l* thick; (D) PPVbPI57-HMW annealed at 160 °C, 6.2*l* thick. The height scale for all images is 50 nm, and the phase scale for all images is 30°.

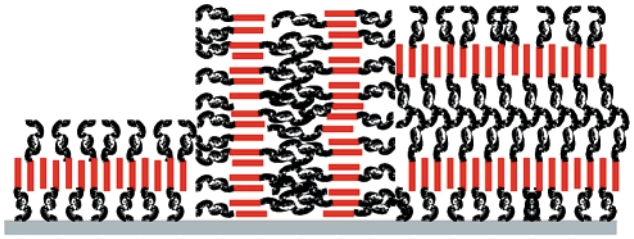

Figure 2. Schematic illustration of parallel and out-of-plane orientations. Lamellar nanodomains are oriented both parallel to the substrate and out of the plane of the film (drawn here in a perpendicular orientation). Parallel regions appear featureless in SFM images due to structural symmetry in the plane of the film, whereas lamellae with out-of-plane symmetry appear as alternating light and dark stripes in the phase image due to differences in mechanical properties between the PPV and PI nanodomains. In regions of parallel orientation the block copolymer molecules are expected to be oriented roughly perpendicular to the surface, whereas in regions of out-of-plane orientation the molecules lie approximately parallel to the surface.

spacing of the block copolymer as measured by SAXS and SFM. By using a block copolymer containing a hydrogenated PPV block and a deuterated PI block, the depth-dependent concentrations of PPV and PI are determined on the basis of the relative abundance of deuterium and hydrogen nuclei through the depth of the film.

Results and Discussion

Microphase Structure in Thin Films. Nearly symmetric rod−coil block copolymers form lamellar microphase-separated structures in thin films, similar to their structure in the bulk. SFM images, shown in Figure 1, clearly illustrate the rod- and coil-rich nanodomains. Lamellae are oriented both parallel to the substrate and out of the plane of the film. These structures form both in smooth films and in films where island or hole formation is observed. In the phase images, regions of alternating light and dark strips show the edges of lamellae oriented roughly perpendicular to the sample surface. Contrast in the phase images derives from mechanical property differences between the PPV and PI blocks in the copolymers. The PI-rich regions are softer and more adhesive than the PPV-rich regions, generating a phase shift between the different nanodomains. The PPV microphase appears as the light microphase in the phase image, and the PI appears as the dark microphase. Differences in adhesion also affect the height image; the adhesive PI surfaces tend to appear higher than the nonadhesive PPV surfaces in tapping mode due to damping of cantilever oscillations. Featureless regions in the phase images much larger than the 10−20 nm length scale of microphase separation must contain both PPV and PI nanodomains. These featureless regions are grains of lamellae oriented parallel to the substrate, and no structure is visible due to the lamellar symmetry in this plane. Height images indicate that the film thickness in the parallel regions is similar to that in the rest of the film. Since the PI block selectively segregates to the vacuum interface, the lamellar regions oriented parallel to the substrate appear similar in phase contrast to the PI nanodomains in the microphases with out-of-plane orientation.

The out-of-plane lamellae are predominantly oriented perpendicular to the film surface in weakly segregated block copolymers, as demonstrated by GISAXS. The GISAXS pattern for a 140 nm thick film of PPVbPI42-LMW, shown in Figure 3a, has scattering peaks only along the q_z and q_{xy} axes. Peaks along q_z originate from lamellae oriented parallel to the film,[47] while peaks along q_{xy} are from perpendicularly oriented lamellae. The lack of scattering intensity in any other direction indicates a strong preference for microdomain orientation either parallel or perpendicular to the substrate. This bimodal orientation is schematically illustrated in Figure 2. Line cuts through the two-dimensional image show peaks consistent with lamellar structure, as illustrated in Figure 3b. The horizontal cut, taken at a q_z value equal to the q for specular reflection, shows a single peak at 0.0430 1/Å, consistent with the domain spacing observed in the bulk (13.9 nm in bulk vs 14.6 nm in the film).[14] The vertical cut shows a peak at 0.0571 1/Å and a second-order reflection at 0.1037 1/Å. Because of distortions of the X-ray momentum vector inside the film, domain spacings must be calculated within the distorted wave Born approximation (DWBA).[45,47] The low-q peak corresponds to the primary reflection from lamellae with a spacing of 14.1 nm, and the high-q peak corresponds to the secondary reflection from

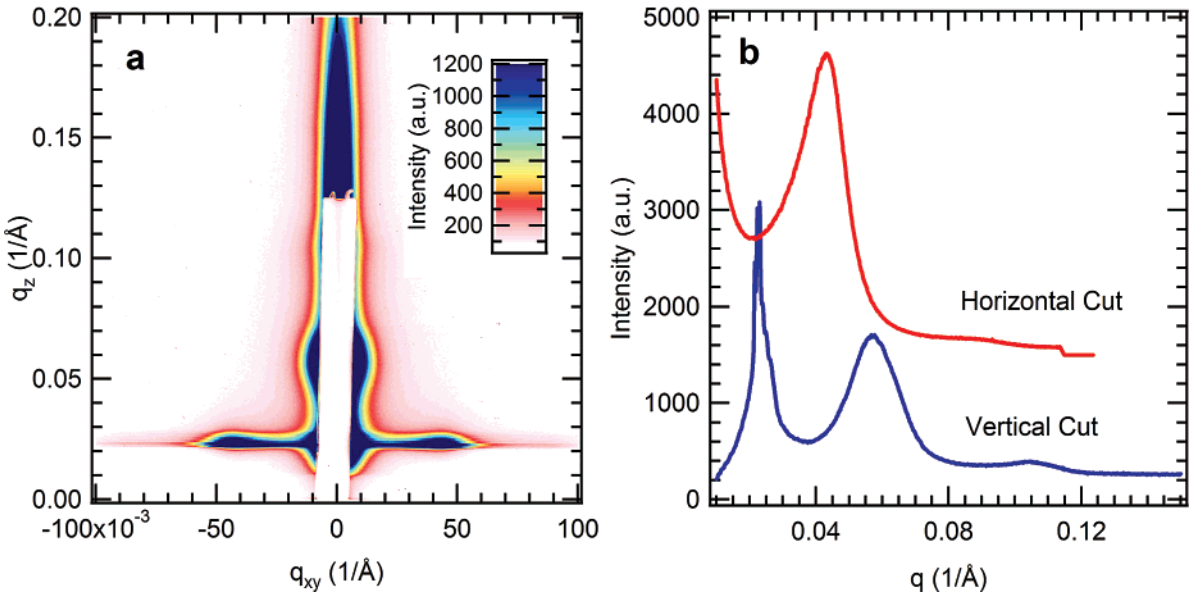

Figure 3. Alignment of lamellar structure in thin films. (a) A GISAXS scattering pattern taken above the critical angle for PPVbPI4-LMW shows scattering peaks only in the q_z and q_{xy} directions, indicating that the out-of-plane lamellae are oriented perpendicular to the film surface and the surrounding in-plane lamellae. The film thickness is 10.0l, and the X-ray incident angle is 0.175°. (b) Line cuts taken from the two-dimensional image illustrate peaks consistent with the lamellar structure. Cuts were taken in the horizontal direction at $q_z = 0.0231$ for specular reflection and in the vertical direction at $q_{xy} = 0.0118$ near the beam stop. The horizontal cut has been offset for clarity.

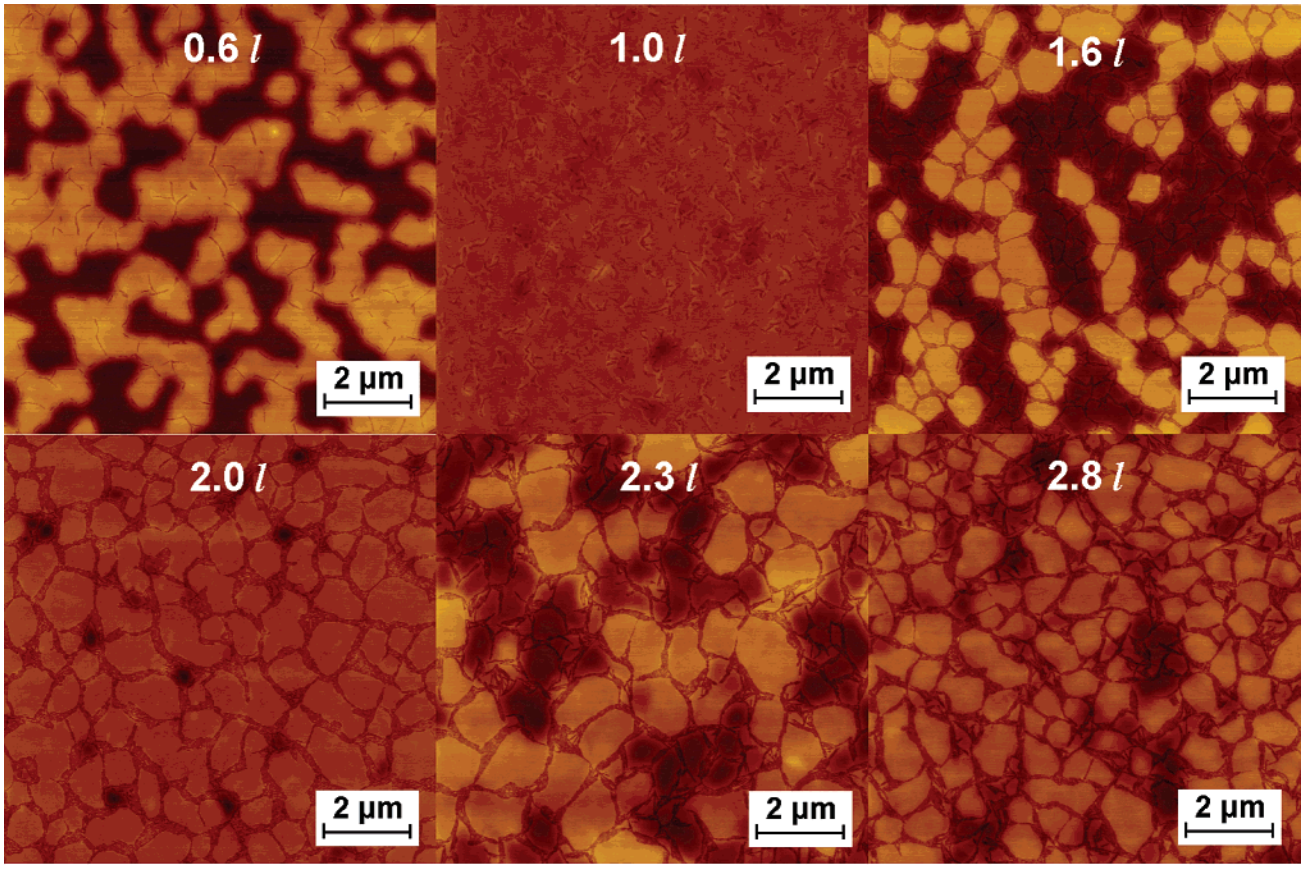

Figure 4. Islands or holes in symmetric rod−coil block copolymer thin films. SFM height images of PPVbPI42-LMW show that rod−coil block copolymers cast into films form islands or holes due to incommensurability between the initial film thickness and the natural domain spacing of the block copolymer. Even deviations of the initial film thickness as small as 2 nm (15% of the domain spacing) from an integer multiple of the natural domain spacing will result in island or hole formation. On the basis of the height of islands or holes, the thin film domain spacing for this block copolymer is estimated to be 14.0 nm, very close to the bulk domain spacing measured by SAXS. The film thickness, normalized by the bulk domain spacing, is listed on each height image, and the *z*-scale for all images is 50 nm.

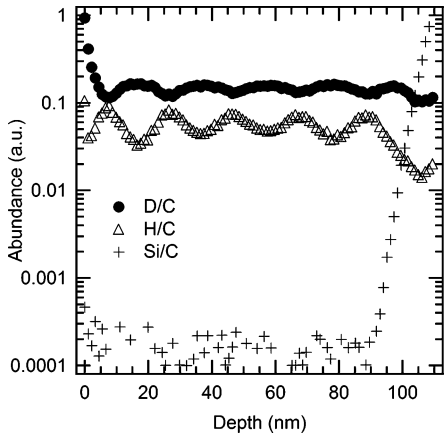

Figure 5. SIMS depth profile for PPVbdPI58-HMW. Depth profiling of a lamellar block copolymer film (with a deuterated polyisoprene block) with predominantly parallel microdomain orientation shows that polyisoprene selectively segregates to both the vacuum and silicon interfaces. Both interfaces show a peak in the deuterium signal, indicating that there is an enrichment of the polyisoprene block at the interfaces. Five peaks are observed in the hydrogen signal, confirming that the film is five lamellae thick.

lamellae with a spacing of 13.7 nm. Both of these estimates of the thin film lamellar spacing are in close agreement with the bulk value.

The perpendicular lamellae are straighter and have a longer persistence length than typical coil−coil block copolymer lamellae, although bending does occur at a few defects, as observed with SFM. Higher molecular weight block copolymers show both better orientational ordering between neighboring lamellae and nanodomains of longer length than lower molecular weight polymers of a similar coil fraction. Similar to TEM observations of PPV-*b*-PI polymers,[14] defects are characterized by breaking rather than bending of the nanodomains. A close examination of the lamellae oriented out of plane in Figure 1 suggests variations in the width of single lamellar nanodomains in most regions with perpendicular orientation. These undulations in lamellar width appear to be favored to fill space in poorly ordered regions of the film. Consistent with this, the thickness variations are more pronounced in the low molecular weight samples that are more weakly segregated and also have a slightly higher rod block polydispersity.

Dislocations and disclinations in block copolymer films can be used to quantitatively estimate the elastic constants of the nanodomains in large grains with isolated defects. Although these rod−coil films do not demonstrate the large grains and isolated defects that make quantification of the elastic constants possible, it is possible to make qualitative conclusions based on the type of defects observed. In coil−coil block copolymers, the modulus for molecular splay is much lower than the nanodomain compressibility of the block copolymers (the ability to change domain spacing), resulting in long wavelength undulations in domain orientation but little variation in domain width.[48] In contrast, the rod−coil systems show discrete variations in lamellar width but no variation in orientation along the length of a lamellae. Since the nanodomain compressibility of a rod−coil block copolymer is dependent upon the segmental interaction and chain stretching free energies which have similar

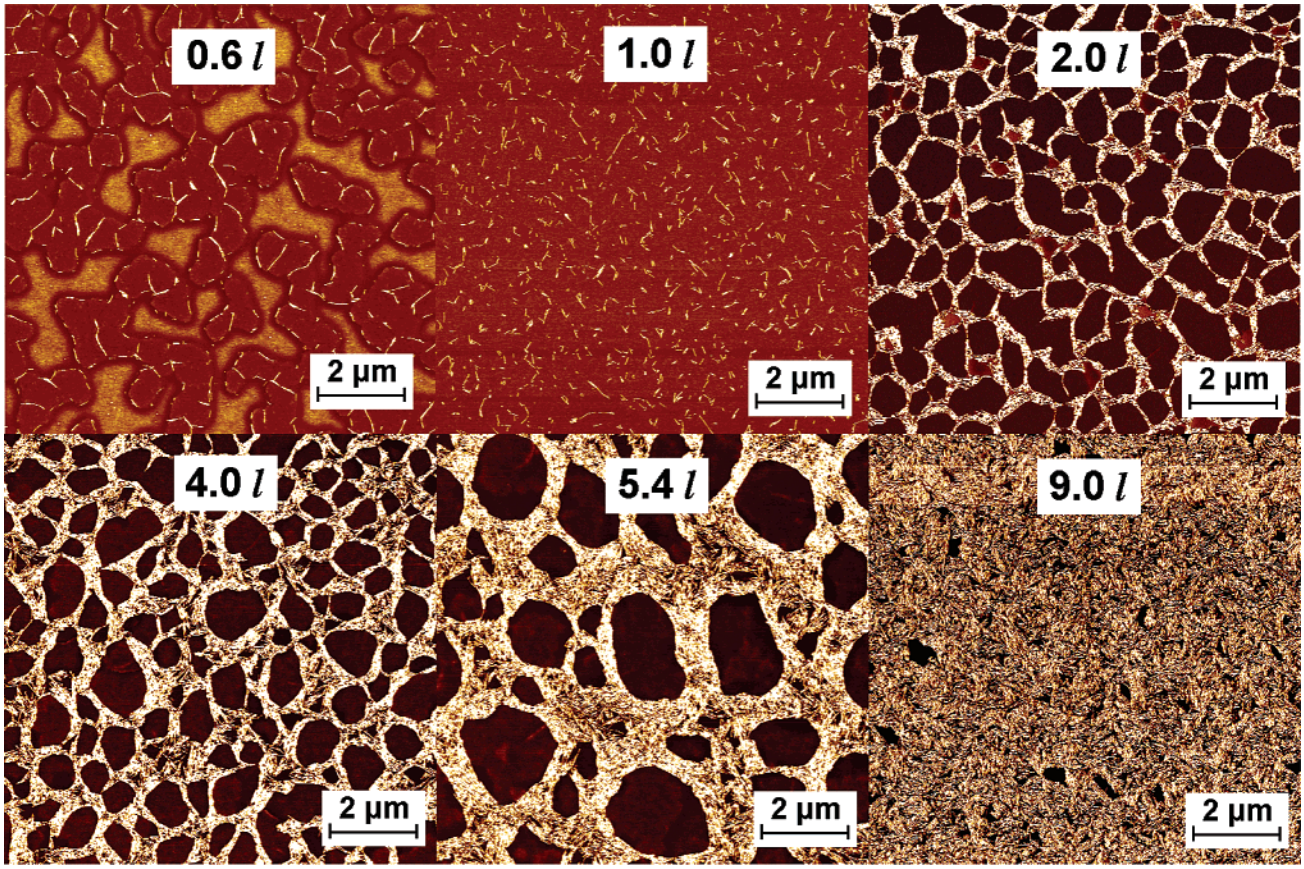

Figure 6. Surface reorientation with increasing film thickness in PPVbPI42-LMW. Increasing film thickness results in a change in microdomain orientation from predominantly parallel to the substrate to predominantly out of the plane of the film. The silicon interface strongly prefers the polyisoprene block, creating a surface orienting effect that propagates into the film. The vacuum interface is weakly preferential for the isoprene block, so lamellae at this interface may take an out-of-plane orientation when they are far enough away from the silicon interface. The film thickness, normalized by the bulk domain spacing, is listed on each phase image, and the *z*-scale for all images is 30°.

magnitudes in weakly segregated rod−coil and coil−coil systems,[9,49] compressibility is expected to be similar for coil−coil and rod−coil block copolymers. Therefore, the splay modulus of the rod−coil material must be significantly higher than in coil−coil block copolymers to produce the variable width lamellar structures. This is not suprising given that the splay energy is correlated to the liquid crystalline rod−rod interaction. Also, in coil−coil block copolymers the rate of change of nanodomain orientation around a disclination gives information on the ratio of the bending modulus to the splay modulus.[48] Since PPV nanodomains break at disclinations, they change direction at an infinite rate at discrete positions, suggesting a ratio of the bending modulus to the splay modulus that is much larger than unity. Bending and splay create distortions in liquid crystalline systems that carry large energetic penalties, so the high moduli of the PPV nanodomains result from the aligning liquid crystalline interactions between the rod blocks.

Grains with lamellae oriented parallel to the silicon substrate grow into irregular shapes, as illustrated in Figure 1. The grains have straight edges defined by lamellar nanodomains with a perpendicular orientation. This irregular polygon shape is the only grain shape observed in these rod−coil polymers for all coil fractions studied, and the grain shape is independent of film thickness. Higher annealing temperatures or longer annealing times result in larger grains of a similar shape. This is in strong contrast with coil−coil block copolymers where grains in bulk samples grow into elliptical shapes that minimize the surface energy of the grain,[50] and thin films also show grain structures with rounded edges.[51] In the case of rod−coil block copolymers, the long persistence length and high bending modulus of the bounding out-of-plane lamellae enforce straight edges on the grains. However, surface energy considerations would like to minimize the grain boundary area. A compromise between these two effects results in the formation of several straight sides to form an irregular polygon. When the number of sides is large, these polygons approximate the elliptical shape observed in coil−coil block copolymers.

Islands and Holes in Rod−Coil Block Copolymers. Rod−coil block copolymer thin films form islands or holes due to incommensurability between the film thickness and the natural domain spacing of the block copolymer. Figure 4 shows height images for a series of film thicknesses of PPVbPI42-LMW. The film thicknesses have been nondimensionalized in terms of the lamellar period (measured by SAXS on a bulk sample) in order to indicate the number of lamellar layers covering the surface. As the film thickness is increased, the film alternates between smooth and uneven surfaces, with smooth surfaces occurring for films with thicknesses equal to an integral number of domain spacings. Even very small deviations in thickness (less than 2 nm) from an integer multiple of domain spacings result in islands or holes, indicating that the formation of additional interface is strongly preferred over a change in block copolymer domain spacing either by rod tilt or coil stretching to accommodate the thickness incommensurability. The heights of island or hole layers, shown in Table 1, are very close to the bulk domain spacings measured by SAXS, indicating that the islands and holes differ in height by a single lamellar domain and that the domain spacing of parallel oriented lamellae is the same in the film as in the bulk.

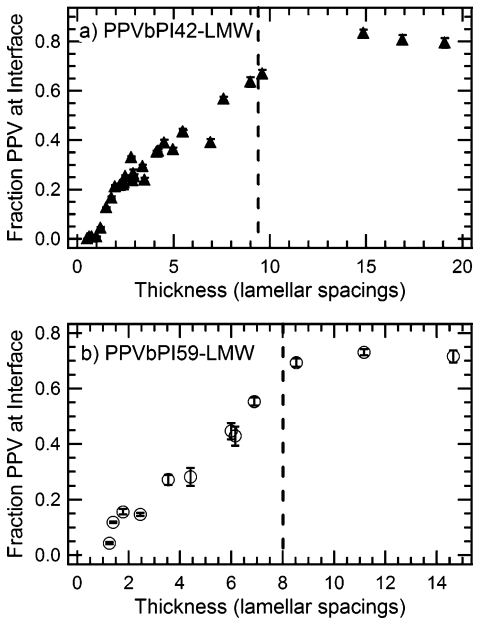

Figure 7. Graphs of surface reorientation as a function of film thickness. Quantitative analysis of SFM phase images shows a steady increase in the fraction of PPV nanodomains (light phase) visible at the polymer/vacuum interface. This indicates that reorientation of the lamellar microdomains occurs continuously as thickness is increased until a plateau value of PPV nanodomains is reached at the vacuum interface. Dashed lines indicate the qualitative reorientation point as determined from the SFM images. (a) Plot for PPVbPI42-LMW shows total reorientation at ~9 lamellar periods with a plateau PPV nanodomain fraction at the vacuum interface of ~80%. (b) Plot for PPVbPI59-LMW shows reorientation at 8 lamellar periods and a plateau PPV nanodomain fraction at the vacuum interface of ~70%.

While the total area covered by islands or holes is an equilibrium phenomenon, their growth and size are kinetic properties. The fraction of high regions is a function of the excess film thickness above an integer multiple of domain spacings; increasing the excess film thickness results in an increased amount of the high level until the next smooth condition is reached. Different patterns of islands or holes are observed at different film thicknesses. With increasing excess film thickness isolated islands, interconnected networks of high and low regions, and isolated holes are observed. While increasing annealing temperature leads to larger islands or holes, it does not change the characteristic island or hole pattern.

The parallel domain orientation necessary to generate a dimensional incommensurability in lamellar systems is caused by selective segregation of one block to either or both of the film interfaces. For PPV-*b*-PI block copolymers, the isoprene block prefers both the native oxide and the vacuum interface, resulting in a symmetric wetting condition as determined by dSIMS (Figure 5). Oscillations in hydrogen and deuterium content due to lamellar ordering of the block copolymer parallel to the substrate are clearly evident. The deuterium count has peaks at both the vacuum and oxide interfaces, indicating that the low surface energy isoprene block selectively segregates to both surfaces. Symmetric wetting is consistent with the observation of smooth films at integer multiples of the bulk domain spacing.

The grain structures of the films are closely related to the growth of islands or holes. Regions of perpendicularly oriented lamellae mediate most of the island or hole boundaries shown in Figure 4. These perpendicular lamellae at the grain boundaries are not required to have a quantized height, so they accommodate the thickness transition between island or hole regions and the surrounding area. The abundance of perpendicularly oriented lamellae subdividing island or hole regions suggests that these defects are also kinetically trapped between grains within a single island or hole.

Surface Reorientation in Thicker Films. The finite penetration of surface ordering fields into the film causes microdomain orientation to change with increasing film thickness. As film thickness is increased, the structures observed at the vacuum interface change from being predominantly parallel oriented lamellae to entirely perpendicularly oriented lamellae. Figure 6 shows this phenomenon with increasing thickness for PPVbPI42-LMW. Reorientation of the lamellae may be quantitatively estimated by calculating the percent of light (PI) nanophase in the SFM phase images, and this data is plotted as a function of thickness in domain spacings for PPVbPI42-LMW in Figure 7a. The images and quantitative area estimates clearly show that the fraction of perpendicular lamellae increases steadily until the entire film is in the perpendicular orientation, at which point the amount of white space reaches a saturation plateau. This reorientation effect is due to the interplay between surface-induced orientation fields and the kinetics of lamellar structure formation, and a similar mixed orientation has been observed in coil−coil systems with one preferential and one neutral surface.[18] Early in the annealing process, diffusion of the block copolymers on the length scale of a single domain results in microphase separation into lamellar domains. Polymers close to the interfaces feel their effects, and these aligned grains tend to propagate into the film. The silicon interface appears to have a strong surface orienting effect that can propagate all the way through thin films. The vacuum interface has a weaker surface preferential effect, so when this interface is sufficiently far from the silicon substrate, perpendicular orientation results due to the nucleation of grains independently of the strong surface field. Pereira and Williams' model suggests that this reorientation may be more favorable in rod−coil systems than coil−coil systems, and it may serve to relax some of the incommensurability in thicker films.[42]

Changing coil fraction or annealing temperature affects how far the surface-ordering field from the Si interface penetrates into the film. Increasing coil fraction increases the disorder within the lamellae, so the transition to a fully out-of-plane surface orientation occurs with fewer lamellar thicknesses. For PPVbPI42-LMW this plateau occurs at ~9 domain spacings, while for PPVbPI59-LMW the plateau occurs at 8 domain spacings, as shown in Figure 7. However, in terms of absolute film thickness PPVbPI59-LMW undergoes the transition at a much larger thickness due to its larger domain spacing. Increasing the annealing temperature results in the formation of more parallel lamellae and a shift of the reorientation thickness to higher thickness due to a decrease in kinetic barriers to domain reorientation, as shown in Figure 8. In these mixed orientation films, the perpendicular lamellae are kinetically trapped. Increasing annealing temperature or annealing time (over short time periods) increases the fraction of parallel lamellae, but the time to achieve a completely parallel orientation is not experimentally achievable. While annealing above the ODT and recooling would likely result in complete parallel orientaiton, it is not possible to anneal above the ODT due to dewetting of the films on the Si substrates.

Significant interfacial roughness is still observed at the polymer/vacuum interface in films thicker than the reorientation transition, presumably due to kinetic trapping of microdomain orientations. Because there is no thickness quantization in

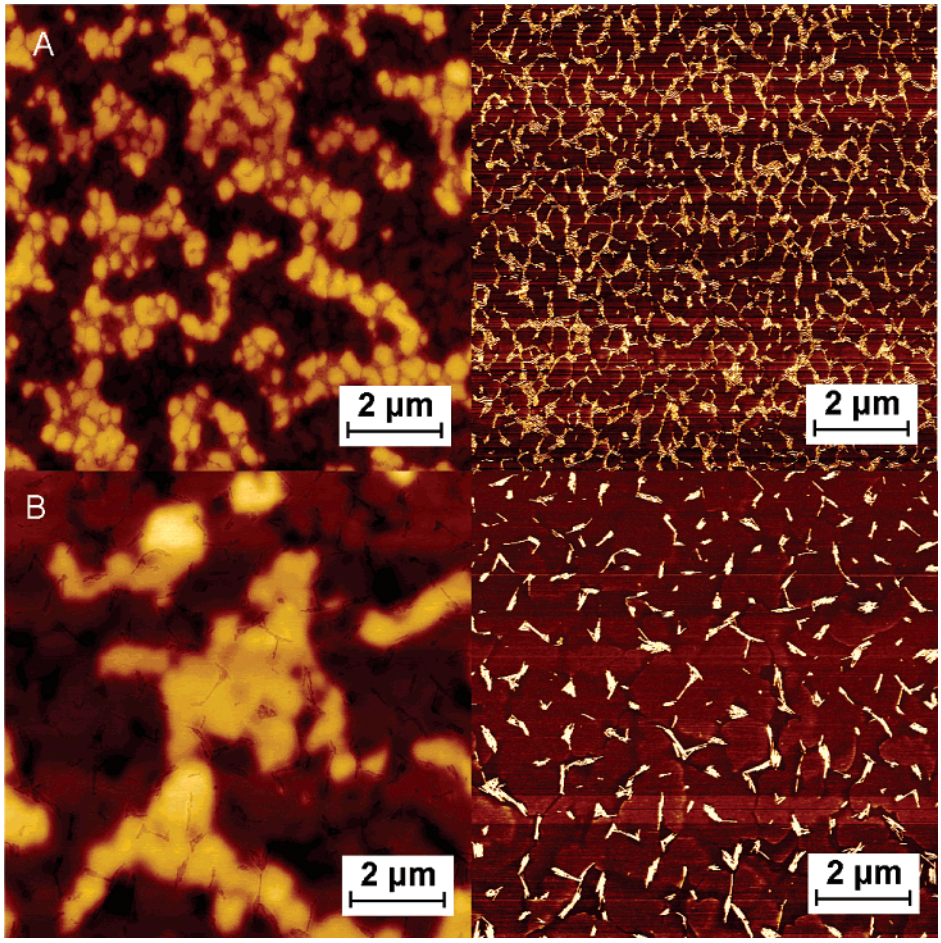

Figure 8. Effect of temperature on grain size and nanodomain orientation. Increasing the annealing temperature results in an increase in grain size; however, grain shapes remain qualitatively similar. Increasing annealing temperature also results in the fraction of nanodomains at the vacuum interface with a parallel orientation, as shown qualitatively by the phase images. (A) annealed at 120 °C; (B) annealed at 160 °C. The scale for height images (left) is 50 nm, and the scale for phase images (right) is 30°. The film thickness is 4.5*l* for both samples.

perpendicularly oriented lamellae, it would be expected that films with out-of-plane orientation at the interface can accommodate arbitrary film thicknesses without the formation of a rough interface. However, significant interfacial roughness is still observed at thicknesses where all microdomains at the vacuum interface show a perpendicular orientation, and flat conditions cannot be achieved by changing film thickness. A representative 2500 μm^2 area of a 14 l thick film of PPVbPI59-LMW has an rms roughness of 2.55 nm and a *z* range of 24.3 nm. Roughness greater than 10% of the polymer domain spacing is typical for these thick films, but this roughness is not observed on top of flat areas of islands or holes in thinner films. This apparently nonequilibrium situation may result from the kinetic trapping of lamellar microstructure that prevent neighboring grains from communicating. Two neighboring regions may both nucleate grains at the Si interface, and as these grains grow small fluctuations in film thickness result in one forming more layers than the other. However, the large transitional energy between perpendicular and parallel lamellae precludes the parallel lamellae acting as sinks/sources that provide block copolymer mobility for reorientation.

Conclusions

The self-assembly of symmetric rod−coil block copolymers in thin films was studied using a model system of weakly segregated PPV-*b*-PI block copolymers. Because of knowledge of surface wetting conditions and the ODT, this system provides unique insights into the behavior of rod−coil block copolymers in thin films. The PI block preferentially wets both the silicon and the air interface in thin films, although the Si interface shows a much stronger preference for the PI block than the air interface. Thermally annealed films self-assemble into lamellar microphases with both parallel and perpendicular orientations relative to the substrate. Perpendicular lamellae are characterized by a long persistence length and break rather than bend near defects due to the high bending modulus of the liquid crystalline PPV nanodomains. Lamellae with parallel orientation grow into irregular polygon grains with the straight edges bounded by the rigid lamellae with a perpendicular orientation. Incommensurability between the film thickness and the natural period of the block copolymer results in the formation of two-level island or hole structures in films, and the transition between islands or holes and surrounding regions is mediated by defect nanodomains with perpendicular orientation. Increasing film thickness results in an observed domain reorientation at the vacuum interface due to the decaying effect with increasing film thickness of the surface-induced orienting field originating at the silicon interface.

Acknowledgment. We gratefully acknowledge support from the ACS Petroleum Research Fund, a 3M Untenured Faculty Award, and the DOE-BES Plastic Electronics Program at the Lawrence Berkeley National Laboratory. This work made use of the Materials Research Lab Central Facilities at the University of California Santa Barbara supported by the National Science Foundation under Award DMR00-80034. We thank Tom Mates

for assistance with SIMS experiments. GISAXS experiments were conducted at the APS, supported by the U.S. Department of Energy, Office of Basic Energy Sciences, under Contract W-31-109-ENG-38. The authors thank the APS Sector 8 staff for assistance with these experiments. B. D. Olsen gratefully acknowledges the Fannie and John Hertz Foundation for a graduate fellowship.

References and Notes

(1) Segalman, R. A. *Mater. Sci. Eng., R* **2005**, *48*, 191−226.
(2) Fasolka, M. J.; Mayes, A. M. *Annu. Rev. Mater. Res.* **2001**, *31*, 323−355.
(3) Harrison, C.; Dagata, J. A.; Adamson, D. H. Lithography with Self-assembled Block Copolymer Microdomains. In *Developments in Block Copolymer Science and Technology*; Hamley, I. W., Ed.; John Wiley & Sons Ltd.: New York, 2004; pp 295−323.
(4) Moons, E. *J. Phys.: Condens. Matter* **2002**, *14*, 12235−12260.
(5) Voigt, M.; Chappell, J.; Rowson, T.; Cadby, A.; Geoghegan, M.; Jones, R. A. L.; Lidzey, D. G. *Org. Electron.* **2005**, *6*, 35−45.
(6) Yu, G.; Gao, J.; Hummelen, J. C.; Wudl, F.; Heeger, A. J. *Science* **1995**, *270*, 1789−1791.
(7) de Boer, B.; Stalmach, U.; van Hutten, P. F.; Melzer, C.; Krasnikov, V. V.; Hadziioannou, G. *Polymer* **2001**, *42*, 9097−9109.
(8) Lu, S.; Liu, T. X.; Ke, L.; Ma, D. G.; Chua, S. J.; Huang, W. *Macromolecules* **2005**, *38*, 8494−8502.
(9) Pryamitsyn, V.; Ganesan, V. *J. Chem. Phys.* **2004**, *120*, 5824−5838.
(10) Olsen, B. D.; Segalman, R. A. *Macromolecules* **2006**, *39*, 7078−7083.
(11) Chen, J. T.; Thomas, E. L.; Ober, C. K.; Hwang, S. S. *Macromolecules* **1995**, *28*, 1688−1697.
(12) Chen, J. T.; Thomas, E. L.; Ober, C. K.; Mao, G. P. *Science* **1996**, *273*, 343−346.
(13) Radzilowski, L. H.; Carragher, B. O.; Stupp, S. I. *Macromolecules* **1997**, *30*, 2110−2119.
(14) Olsen, B. D.; Segalman, R. A. *Macromolecules* **2005**, *38*, 10127−10137.
(15) Russell, T. P.; Coulon, G.; Deline, V. R.; Miller, D. C. *Macromolecules* **1989**, *22*, 4600−4606.
(16) Krausch, G.; Magerle, R. *Adv. Mater.* **2002**, *14*, 1579−1583.
(17) Mansky, P.; Russell, T. P.; Hawker, C. J.; Pitsikalis, M.; Mays, J. *Macromolecules* **1997**, *30*, 6810−6813.
(18) Huang, E.; Russell, T. P.; Harrison, C.; Chaikin, P. M.; Register, R. A.; Hawker, C. J.; Mays, J. *Macromolecules* **1998**, *31*, 7641−7650.
(19) Huang, E.; Mansky, P.; Russell, T. P.; Harrison, C.; Chaikin, P. M.; Register, R. A.; Hawker, C. J.; Mays, J. *Macromolecules* **2000**, *33*, 80−88.
(20) Xu, T.; Hawker, C. J.; Russell, T. P. *Macromolecules* **2005**, *38*, 2802−2805.
(21) Konrad, M.; Knoll, A.; Krausch, G.; Magerle, R. *Macromolecules* **2000**, *33*, 5518−5523.
(22) Thomas, E. L.; Kinning, D. J.; Alward, D. B.; Henkee, C. S. *Macromolecules* **1987**, *20*, 2934−2939.
(23) Thomas, E. L.; Anderson, D. M.; Henkee, C. S.; Hoffman, D. *Nature (London)* **1988**, *334*, 598−601.
(24) Coulon, G.; Collin, B.; Ausserre, D.; Chatenay, D.; Russell, T. P. *J. Phys. (Paris)* **1990**, *51*, 2801−2811.
(25) Mayes, A. M.; Russell, T. P.; Bassereau, P.; Baker, S. M.; Smith, G. S. *Macromolecules* **1994**, *27*, 749−755.
(26) Leclere, P.; Calderone, A.; Marsitzky, D.; Francke, V.; Geerts, Y.; Mullen, K.; Bredas, J. L.; Lazzaroni, R. *Adv. Mater.* **2000**, *12*, 1042−1046.
(27) Wang, H. B.; Wang, H. H.; Urban, V. S.; Littrell, K. C.; Thiyagarajan, P.; Yu, L. P. *J. Am. Chem. Soc.* **2000**, *122*, 6855−6861.
(28) Leclere, P.; Hennebicq, E.; Calderone, A.; Brocorens, P.; Grimsdale, A. C.; Mullen, K.; Bredas, J. L.; Lazzaroni, R. *Prog. Polym. Sci.* **2003**, *28*, 55−81.
(29) Hempenius, M. A.; Langeveld-Voss, B. M. W.; van Haare, J.; Janssen, R. A. J.; Sheiko, S. S.; Spatz, J. P.; Moller, M.; Meijer, E. W. *J. Am. Chem. Soc.* **1998**, *120*, 2798−2804.
(30) Stupp, S. I.; LeBonheur, V.; Walker, K.; Li, L. S.; Huggins, K. E.; Keser, M.; Amstutz, A. *Science* **1997**, *276*, 384−389.
(31) Surin, M.; Marsitzky, D.; Grimsdale, A. C.; Mullen, K.; Lazzaroni, R.; Leclere, P. *Adv. Funct. Mater.* **2004**, *14*, 708−715.
(32) Chen, J. T.; Thomas, E. L. *J. Mater. Sci.* **1996**, *31*, 2531−2538.
(33) Liu, J. S.; Sheina, E.; Kowalewski, T.; McCullough, R. D. *Angew. Chem., Int. Ed.* **2001**, *41*, 329−332.
(34) Park, J. W.; Thomas, E. L. *Adv. Mater.* **2003**, *15*, 585−588.
(35) Park, J. W.; Thomas, E. L. *Macromolecules* **2006**, *39*, 4650−4653.
(36) Minich, E. A.; Nowak, A. P.; Deming, T. J.; Pochan, D. J. *Polymer* **2004**, *45*, 1951−1957.
(37) Heiser, T.; Adamopoulos, G.; Brinkmann, M.; Giovanella, U.; Ould-Saad, S.; Brochon, C.; van de Wetering, K.; Hadziioannou, G. *Thin Solid Films* **2006**, *511*, 219−223.
(38) Leclere, P.; Parente, V.; Bredas, J. L.; Francois, B.; Lazzaroni, R. *Chem. Mater.* **1998**, *10*, 4010−4014.
(39) Chochos, C. L.; Tsolakis, P. K.; Gregoriou, V. G.; Kallitsis, J. K. *Macromolecules* **2004**, *37*, 2502−2510.
(40) Gunther, J.; Stupp, S. I. *Langmuir* **2001**, *17*, 6530−6539.
(41) Li, H. B.; Liu, Q. T.; Qin, L. D.; Xu, M.; Lin, X. K.; Yin, S. Y.; Wu, L. X.; Su, Z. M.; Shen, J. C. *J. Colloid Interface Sci.* **2005**, *289*, 488−497.
(42) Pereira, G. G.; Williams, D. R. M. *Macromolecules* **2000**, *33*, 3166−3172.
(43) Olsen, B. D.; Segalman, R. A. *Macromolecules*, manuscript in preparation.
(44) Lee, B.; Park, I.; Yoon, J.; Park, S.; Kim, J.; Kim, K. W.; Chang, T.; Ree, M. *Macromolecules* **2005**, *38*, 4311−4323.
(45) Tate, M. P.; Urade, V. N.; Kowalski, J. D.; Wei, T. C.; Hamilton, B. D.; Eggiman, B. W.; Hillhouse, H. W. *J. Phys. Chem. B* **2006**, *110*, 9882−9892.
(46) Segalman, R. A.; Hexemer, A.; Hayward, R. C.; Kramer, E. J. *Macromolecules* **2003**, *36*, 3272−3288.
(47) Busch, P.; Rauscher, M.; Smilgies, D. M.; Posselt, D.; Papadakis, C. M. *J. Appl. Crystallogr.* **2006**, *39*, 433−442.
(48) Harrison, C.; Cheng, Z. D.; Sethuraman, S.; Huse, D. A.; Chaikin, P. M.; Vega, D. A.; Sebastian, J. M.; Register, R. A.; Adamson, D. H. *Phys. Rev. E* **2002**, *66*, 011706.
(49) Leibler, L. *Macromolecules* **1980**, *13*, 1602−1617.
(50) Balsara, N. P.; Marques, C. M.; Garetz, B. A.; Newstein, M. C.; Gido, S. P. *Phys. Rev. E* **2002**, *66*, 052802.
(51) Angelescu, D. E.; Harrison, C. K.; Trawick, M. L.; Chaikin, P. M.; Register, R. A.; Adamson, D. H. *Appl. Phys. A: Mater. Sci. Process.* **2004**, *78*, 387−392.

MA062402I